INTRODUCTION

Sonofusion devices have been shown to produce 50 W of excess heat energy without generating radioactive byproducts, based on calorimetric and mass spectroscopic analyses. When scaled up sufficiently, this transformational new technology is expected to provide a safe source of dispatchable, centralized, renewable power that can be engineered to support any energy-dependent system. The objective of this project is to make and test a device that produces 1 kW of heat energy by linking several of the existing devices together in a series.

The device consists of a 1.6-MHz oscillator-driven piezo resonating in heavy water (D_2O), which induces the formation of millions of transient cavitation bubbles. As detailed in Appendix 1: Related Research, the much-studied phenomenon of cavitation initiates a charge separation that is subsequently enhanced by the z-pinch effect, which has long frustrated Tokamak fusion systems, and the charge separation is further enhanced by the more recently reported image charge phenomenon. In sonofusion devices, the enhanced charge separation is considered to generate a unique set of conditions posited to culminate in a fusion event that diffuses the expected gamma photon via bremsstrahlung radiation. Appendix 2 presents experimental evidence in support of the proposed mechanism.

The next step towards developing sonofusion technology is to produce more heat energy by linking several of these devices together in a series that can be expanded to any desired extent, much like adding strings of lights on a Christmas tree. The materials necessary for the manufacture of the serial devices are quite inexpensive. However, further development requires equipment upgrades, a lab assistant, and independent data analysis and consulting. Based on the budget for these items, this principle investigator respectfully requests a grant of $300,000, to be spent over two years, for the development of this transformational new technology.

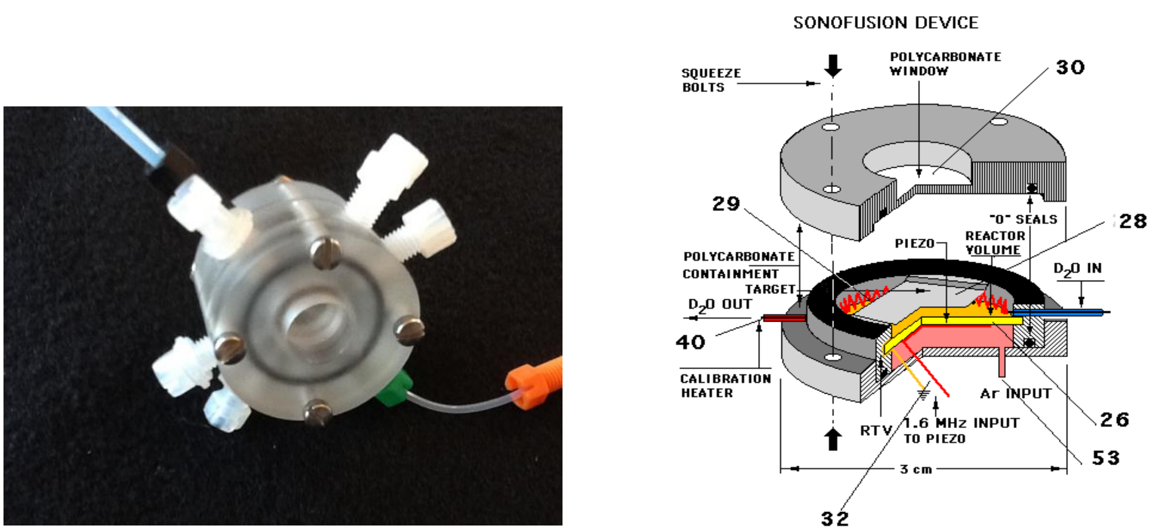

Figure 1. Sonofusion device: digital photograph (left) and schematic (right).

OBJECTIVE

The objective of this project is to make and test a device that produces 1 kW of heat energy by linking several of the existing devices together in a series. Each existing device produces 50 W of excess heat energy. Therefore, to produce 1 kW, this project must connect 20 of the individual units.

Most of the first year of the project will be devoted to achieving the preliminary objective of configuring a stack of four sonofusion units, as illustrated in Figure 2. The thin, flat disc of the piezo provides a favorable geometry for a stacked configuration. Recent tests indicate that the stack should be positioned in line with the flow of D_2O, at a 90º angle to that pictured, to maintain a uniform bubble distribution.

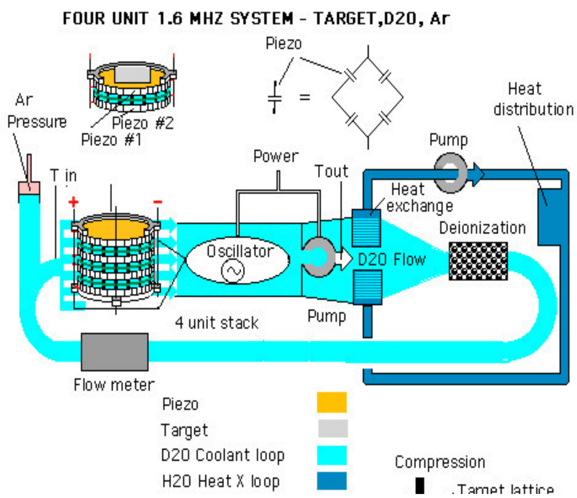

Figure 2. Schematic of one possible configuration of the preliminary four-unit stack.

In the second year of the project, after comprehensive testing and analysis of the four-unit stacks, five of these stacks will be configured in a 20-unit system to achieve the ultimate goal of a 1-kW sonofusion device. Testing and analysis of this 20-unit system, as well as enhanced engineering to maximize its efficiency, will advance sonofusion technology such that it can be engineered for specific applications in the commercial energy market.

PROJECT DESCRIPTION

In the first month of the project, development expenditures will support the hiring of a lab assistant, as described below under Personnel, as well as equipment updates that are required to run and monitor the sonofusion device. As detailed in the Project Budget, below, new equipment is required to complete several circuits that must be constructed to test the device in the laboratory. One circuit circulates light water (H_2O) through the resonator to withdraw heat, and another circuit pressurizes the system with argon (Ar) gas to prevent contamination from atmospheric gases and to collect sample gases for mass spectroscopic analysis. H_2O flowing out of the reactor proceeds first to a bubbler that collects any residual bubbles and pressurizes the H_2O with Ar. From the bubbler, the H_2O runs through a pump that controls the flow rate to the desired level, expelling H_2O in measured increments that then flow through a heat exchanging reservoir and a filter to further purify and calibrate the H_2O before it re-enters the cell.

Another circuit delivers one of two power sources to the device. One input port permits calibration in the absence of cavitation activity by connecting a power supply to a resistance heater in the device that is monitored by a calibration wattmeter. A second power input port activates the piezo: DC power flows through a wattmeter, then a transformer, and into an oscillator, which is connected to the reactor's piezo by wires shielded with ferrite beads to protect the measurements from radiofrequency interference.

These circuits work together to drive the resonator and produce data according to the following experimental method. To conduct an experiment on this system, the DC power input is turned on to begin a run, the reactor temperature is monitored as it approaches and achieves steady state, and the input power is turned off after the reactor has run at steady state for several minutes. The temperature inside the unit is then allowed to cool to the same starting temperature before initiating a calibration run on the given parameter settings by supplying input power to a 60-ohm resistance heater (ARi Industries, Inc.) that is permanently embedded in the reactor chamber. Temperature measurements are obtained from one K-type thermocouple in an aluminum sheath that is inserted in the non-circulating D_2O volume in the reactor chamber, and another K-type thermocouple is located in the 3.5-L H_2O cooling reservoir. The temperature differences are taken from the difference between the thermocouple measurement from the non-circulating D_2O and that from the reservoir, and the temperature differences generated by the running and calibration modes are compared. Differences between the steady state temperatures of the running and calibration modes are considered to indicate excess heat.

In the months after the new equipment has been tested and calibrated, the principle investigator will reconstruct the single sonofusion unit so that four units can be linked to one another in a stacked configuration. These new multi-units will be calorimetrically tested to determine their heat-producing performance and their efficiency in relation to input power. Testing will also include independent mass spectroscopic analysis for nuclear products, as well as scanning electron microscope (SEM) imaging of the device's exposed target foils to investigate the heat-producing mechanism; these independent analyses constitute the bulk of the budget for which funding is requested.

Throughout this testing and modification process, the principle investigator will work towards a four-unit design that facilitates further expansion. By the end of the first year of the funding period, the project will advance to the design and machining of a housing, flow system, and heat exchange system that will accommodate five of the four-unit stacks. An independent machinist will need to be contracted to construct a housing with sufficient capacity to contain the expected heat.

Testing of the expanded 20-unit system is expected to begin in the first months of the second year of the project period. Data from calorimetric testing, mass spectroscopic analysis, and SEM imaging will inform adjustments to the temperature, pressure, and acoustic input parameters to maximize the system's efficiency, with the goal of producing 1 kW of excess heat. Contingency expenditures have been budgeted in case independent consultants need to be contracted to provide expertise on particular temperature distribution or engineering challenges.

In addition to submitting regular progress reports, laboratory personnel will compile comprehensive reports of all data and analysis for expedited use by stakeholders at the conclusion of the funding period.

PROJECT BUDGET

SPENDING CATEGORY	ITEM	COST ($) YEAR ONE	COST ($) YEAR TWO
Personnel	Laboratory Assistant	30,000	30,000
	SUBTOTAL	**30,000**	**30,000**
Equipment Update	Agilent 6035A DC Power Supply	3500	
	Fluid Metering, Inc., Industrial Variable Speed Pump	1500	
	Cole Parmer EW-07061-40 Dry Vacuum Pump	600	
	SUBTOTAL	**5,600**	**0**
Materials	Target foil material (Pd, Ag, Cu, ...)	1800	
	0.50 L D_2O: 99.8%	600	
	SUBTOTAL	**2,400**	**0**
Consulting & Analysis	Mass spectroscopy	52,000	52,000
	SEM imaging	30,000	30,000
	Independent machinist	5,000	15,000
	SUBTOTAL	**87,000**	**97,000**
Transportation	Shipping	3,000	3,000
	Travel	6,000	6,000
	SUBTOTAL	**9,000**	**9,000**
Contingency	**SUBTOTAL**	**15,000**	**15,000**
	ANNUAL TOTAL	**149,000**	**151,000**
	GRAND TOTAL	**300,000**	

PERSONNEL

Principle Investigator Roger Stringham served in the US Army during the Korean War before earning his BS in Chemistry from the University of California (UC), Berkeley. He then joined Stanford Research Institute (SRI), where he worked from 1960 to 1975 on a broad spectrum of research projects, focusing on high resolution magnetic resonance and the development of exotic fluoro-chemical species such as perfluoro ammonium ion. In 1975, he joined Science Applications International Corporation (SAIC), where he helped to found a laboratory in the Sunnyvale, California, SAIC division. His work with SAIC combined fluorine photochemistry and cavitation, focusing on the synthesis of exotic molecules. At both SRI and

SAIC, Mr. Stringham coauthored papers that appeared in numerous journals, including the *Journal of the Association of Official Analytical Chemists*, the *Journal of Chemical Physics*, and the *Journal of Fluorine Chemistry*.

In 1987, Mr. Stringham started a consulting company, Photosonication Consulting, to advance research into photochemistry and cavitation. In 1989, when Martin Fleischmann and Stanley Pons announced their finding of excess heat from an electrochemical cell, Mr. Stringham adapted his cavitation apparatus to include certain features of the Fleischmann-Pons cell, most notably by adding a palladium target foil in the vicinity of the oscillating component. The significant quantities of excess heat that Mr. Stringham observed from this repurposed apparatus stimulated a shift in his research focus that continues to this day.

While the funding agency retains final authority over the selection of the Laboratory Assistant, Mr. Stringham highly recommends Kimberly Nunlist for the position. Ms. Nunlist's BA in Interdisciplinary Studies from UC, Berkeley, is ideally suited to the interdisciplinary nature of this research. In addition, as the author of this proposal, Ms. Nunlist has already become familiarized not only with the research objectives and methods, but also with the actual device and equipment, and would therefore be able to bypass the initial training period that would slow the integration of other candidates.

APPENDIX 1: RELATED RESEARCH

Several independent energy research projects support the science behind the proposed sonofusion device. Although contemporary experimental fusion systems have shown varying degrees of success, they each have certain weaknesses that sonofusion systems either avoid or use to their advantage.

MUON FUSION AND CRITICAL PARTICLE DENSITIES

Experiments in muon fusion have set a standard for particle densities in other fusion systems, although muon fusion itself is not a practicable energy source. Muons are among the most elementary particles in nature, with the same negative electrical charge as the electron but 207 times heavier. The muons' negative charge allows them to take the place of electrons in a deuterium molecule; however, because muons are so much heavier, they orbit 207 times closer to the nuclei of the two atoms in the molecule. This brings those nuclei so close that the atoms fuse, releasing neutrons and helium.

Muon fusion will never be an economical energy source because the process relies on a large particle accelerator, requiring much more energy input than can possibly be recovered. Nonetheless, the well-documented success of muon fusion, especially at low temperatures, proves that deuterium atoms will fuse in systems with densities of 10^{36} particles per cubic meter, which sets a quantifiable standard for particle densities at low temperatures in other fusion systems [1]. The sonofusion device is considered to reach these densities through three stages of compression: the collapsing cavitation bubble, the resultant z-pinch jet, and the trapped deuteron cluster.

THE CAVITATION BUBBLE

The sonofusion process begins with an acoustic piezo, resonating in heavy water to produce a transient cavitation bubble environment. Because of the damage cavitation causes to ship propellers, pump impellers, and other equipment used in the industrial movement of liquids, the cavitation process has been much studied and is well-documented [2]. Bubbles originate in a low-pressure environment, induced by relevant equipment in industrial settings, or by the resonating piezo in sonofusion systems. As the bubble expands in the low-pressure isothermal growth stage, it picks up vapor mass from the bubble's interface. Progressing, the acoustic pressure passes into the positive pressure zone of the acoustic wave, where the partially evacuated bubble reaches its maximum radius, at which point it starts its sub-microsecond collapse.

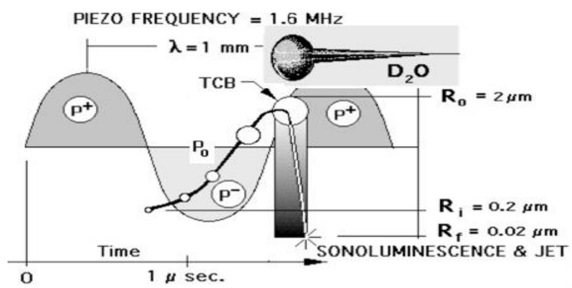

Figure 3. Growth and collapse of a cavitation bubble: the selected initial bubble with radius (R_i) grows isothermally, increasing in mass until its radius reaches a maximum (R_o), at which point the bubble collapses adiabatically to a final radius (R_f), producing sonoluminescense and a high-density jet.

The bubble's energy density increases tremendously during its collapse. Figure 3 describes one bubble's growth and collapse over the course of one acoustic cycle. Each cycle of a piezo resonating at 1.6 MHz produces millions of bubbles with an initial radius (R_i) of around 0.2 μm, which expand to a maximum radius (R_o) of 2 μm, and then collapse to a final radius (R_f) of 0.02 μm. This hundred-fold decrease in the bubble's radius, together with the increase in the bubble's mass content in the low-pressure phase, results in a one million-fold increase in the bubble's energy density. This energy is enough to dissociate some of the D_2O in the bubble contents.

In the collapse, the bubble's surface accelerates towards its center at Mach 10 velocity; a burst of photons is emitted as sonoluminescence; and the plasma contents of the bubble are subsumed within what is known as a z-pinch jet [3].

THE Z-PINCH JET

The z-pinch jet consists of a high-density deuteron plasma confined and compressed by the electromagnetic pressure of a sheath of electrons carried over from the bubble's interface [4–6]. The electromagnetic pressure exerted by the electron sheath around the deuteron plasma accelerates the jet's speed and reduces its radius, further compressing the deuteron plasma to even higher densities. In the absence of intervention, this pressure will narrow the jet's radius until it disintegrates entirely.

This effect has frustrated teams of scientists throughout the world in their efforts to initiate fusion by continuously circulating a hot plasma of deuterons, electrons, and tritons in Tokamak-like devices [7]. These systems are large, doughnut-shaped devices, where the thickness of the ring is approximately ten feet and the total diameter is over 40 feet. As the plasma flows around the ring, it generates an electromagnetic force that compresses the plasma to increasingly higher densities, releasing excess heat energy in the process. However, the Tokamak torus generates energy for only a few milliseconds before the electromagnetic force of the z-pinch jet pinches off the plasma flow entirely. The teams of scientists developing these systems have devoted considerable effort to obtaining a pinch effect that would generate energy without terminating the plasma flow; they have not yet been able to surmount this obstacle.

Sonofusion systems overcome the Tokamak limitation by locating a target foil lattice such that the z-pinch jet, with its compressed deuteron plasma, implants the lattice before the jet is fully terminated.

IMAGE CHARGES AND THE DEUTERON CLUSTER

When the z-pinch jet hits the target lattice, the local lattice of approximately 20 atoms becomes plasma. The heavier, less mobile deuterons from the jet's center form a cluster near the surface. The much more mobile electron sheath forms a spherical cloud of electrons that are attracted by image forces to the positively-charged cluster.

Image forces refer to attractive forces of picosecond duration between one particle and its similarly charged neighbor's image, reflected on the opposing side of an interface between surface charges with large dielectric differences. N. M. Lawandy has reported that these image forces can squeeze deuteron clusters to separations below angstrom dimensions, 10^{-10} m [8]. Image forces are strongest when the permittivity on one side of the interface (ε) is much higher than the relative permittivity on the other (ε_s), i.e., when the permittivity factor $(\varepsilon - \varepsilon_s) / (\varepsilon + \varepsilon_s) = \beta = -1$.

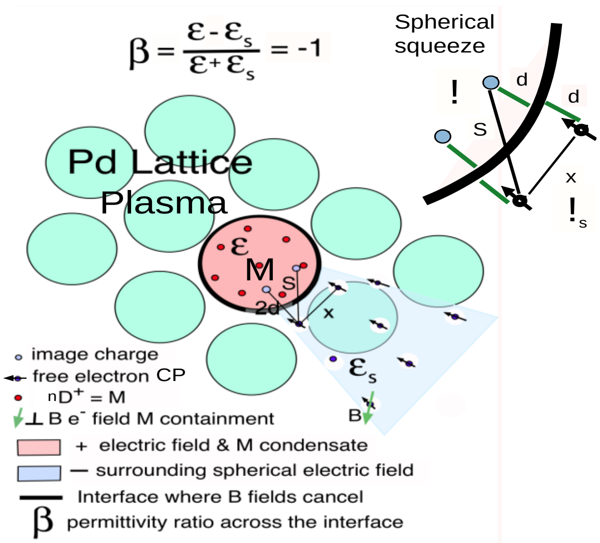

Figure 4. Cooper pair electrons exerting image force attraction on a deuteron cluster in a palladium lattice, with detail of the dimensions involved in calculating image charge for a single Cooper pair at the interface in the upper right corner.

The implantation of the compressed plasma at this stage in the sonofusion process provides exactly the type of environment in which the attractive image forces of like charges are likely to decrease the deuteron particle separation, as shown in Figure 4. The deuteron cluster, already compressed to the relevant densities by the z-pinch jet, becomes trapped near the surface of the lattice and is surrounded by a cloud of highly mobile electrons. The ratio of the permittivities of the deuterons and electrons (ε_s:ε) is 10^3, yielding the ideal permittivity factor, $\beta \approx -1$. Thus, image forces combine with the ordinary attraction between electrons and deuterons, overcoming repulsive forces to compress the deuteron cluster to a density that can reasonably be expected to match that of the muon fusion case.

APPENDIX 2: EXPERIMENTAL EVIDENCE OF SONOFUSION

Even the earliest sonofusion designs promised transformational potential for future energy technologies, when experimental evidence of both excess heat and nuclear products indicated the occurrence of fusion events. Data from those first experiments also suggested ways in which sonofusion technology could be refined to be even more efficient. The most current device produces almost the same amount of heat energy as the earlier designs, but is small enough to fit in the palm of one's hand, and would cost less than $10 per unit when produced in commercial quantities.

TESTING FOR RADIOACTIVITY

The initial designs used piezos resonating at 20 kHz in closed devices of D_2O circulating through a 30-mL reactor pressurized with Ar. In 1993 and 1994, Drs. Tom Claytor and Dale Tuggle at Los Alamos National Laboratory (LANL) assisted in tests including radiation measurements on one of these early sonofusion reactors. None of the equipment deployed to detect radiation, including Geiger and BF_3 counters and a scintillation detector, recorded statistically significant levels of radiation.

TESTING FOR HELIUM PRODUCTION

In 1994, The Electric Power Research Institute awarded a grant of $10,000 for mass spectroscopic analysis of the 20-kHz device. Helium measured in the predicted proportion, with no measurable neutrons or gammas, would indicate that the proposed model followed a possible operative mechanism for the energy release. Scientists at LANL collected gases from the reactor in 50-mL stainless steel volumes, and shipped them to the US Department of Energy's Rocketdyne facility for analysis.

Dr. Brian Oliver at the Rocketdyne facility conducted six trials. Two of these served as standardization samples. One had a standardized amount of ^{4}He in it, to verify the accuracy of the equipment at the Rocketdyne facility. The other was a sample of the Ar gas used to pressurize the device, to ensure no helium was introduced from this outside source.

Two of the trials had measurable products. The sample from the trial with the palladium lattice yielded ^{4}He in the proportion that is predicted by the proposed model. The other sample was from a device with a titanium lattice, tested as an alternative lattice material. This sample revealed the helium isotope tritium, which decayed to ^{3}He, again in the proportion that would be expected from the proposed mechanism.

The last two trials did not measure any helium products, but they were from experimental runs that had not produced excess heat either. This further confirmed the accuracy of the experimental equipment and indicated that the helium and excess heat measured in the previous trials were products of the same event.

The reason these two trials failed to produce excess heat is expected to be that the induced bubbles did not collapse sufficiently quickly to produce the electromagnetically charged jet that forces the deuteron cluster and electron cloud into the target lattice. This problem can be resolved by adjusting temperature, pressure, and acoustic input parameters in response to changes in the cavitation environment to ensure efficient cavitation.

Therefore, subsequent versions of the device have included a multi-pixel photon counter (C13366-3050GA, Hamamatsu Photonics, Inc., Japan) to measure sonoluminescence, the amount of light produced by the collapsing bubbles. The photon counter works in tandem with a feedback mechanism that adjusts the resonating frequency of the oscillator to maximize cavitation efficiency. The feedback mechanism works like a tuning fork, striking the piezo after every cycle to determine what frequency will keep the energy density of cavitation at its highest. Data from the photon counter that measures sonoluminescence corroborate the efficacy of this feedback mechanism in producing cavitation efficiency, and together, these innovations have eliminated the intermittent cavitation failures that plagued earlier sonofusion devices.

SCANNING ELECTRON MICROSCOPE (SEM) IMAGES

SEM images of the earlier device's target foils suggested increasing the frequency of the piezo as another approach to improved efficiency. Figures 4a through 4f show SEM images of the target lattice from a 46-kHz device, produced and tested in 1994. These figures show sites at which the collapsing bubble's jet had driven into the lattice, where the jet's contents were electromagnetically squeezed. These figures also show that the magnitude of target foil damage is related to the piezo's acoustic driving frequency.

Whereas a z-pinch jet implantation may produce several hundred ejecta sites, the size of the ejecta site is relative to the number of fusion events per bubble. Surveys of ejecta sites from these and other SEM images of the 4-kHz device showed a multitude of ejecta sites indicative of 100 or more fusion events per bubble, in contrast to the 20-kHz device, which showed ejecta sites fewer in number but larger in size, up to ten μm across, indicative of up to one million fusion events. Nonetheless, the two devices produced the same amount of heat energy because the higher frequency generated so many more event-producing clusters than the lower frequency. The higher frequency was also less destructive of the target foils, and experiments with the 46-kHz device encouraged further frequency increases in contemporary designs.

(a) 20 kHz; scale: 0.5 mm = 10μm

(b) Detail of Fig. 5a; scale: 1 cm = 1 μm

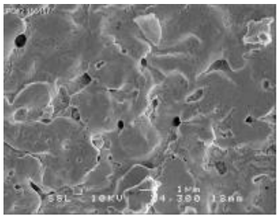

(c) 46 kHz; scale 1 mm = 1µm

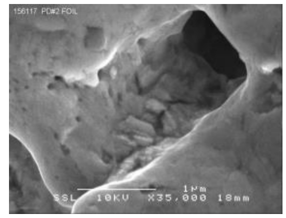

(d) Detail from Fig. 5c; scale: 1 cm = 1 µm

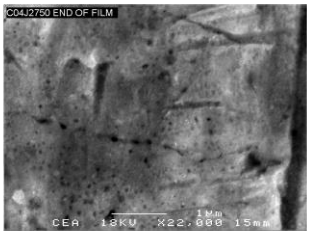

(e) 1.6 MHz; scale: 0.5 cm = 1µm

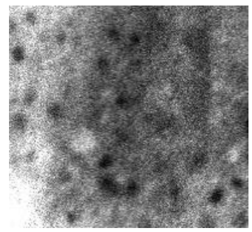

(f) Detail from Fig. 5e; scale: 1 mm ≈ 1 nm

Figure 5. SEM images of target foils exposed at different frequencies: the different sizes of the ejecta sites indicate different numbers of events occurring per implantation. (Image credit: Drs. John Dash and Jane Wheeler)

The latest devices demonstrate a remarkable operating improvement. Figures 4e and 4f above show ejecta site diameters of 50 nm, equivalent to an energy release of approximately 20 million electron volts (MeV). Given that the ejecta site sizes are impossible to measure precisely, these approximations are sufficiently near 24 MeV to indicate the release of one ^4He, signaling the occurrence of a single fusion event. Surveys of the ejecta sites in these SEM images showed that the average energy density of the bubbles in the new device is essentially the same as that of the bubbles in the older device. Thus, the higher frequency of the latest device produces equivalent excess heat energy with less damage to the target lattice.

REFERENCES

[1] LW Alvarez, et al. "Catalysis nuclear reactions by µ mesons." *Phys. Rev.* **105**, 1957.

[2] MP Brenner, S Hilgenfeldt, D Lohse. "Single bubble sonoluminescence." *Rev. of Modern Phys.* **74**, 2002.

[3] KR Weninger, PG Evans, SJ Putterman. "Time correlated single photon Mie scattering from a sonoluminescing bubble." *Phys. Rev. E* **61**, 2000.

[4] Y Tomita, A Shima. "High speed photographic observations of laser induced cavitation bubbles in water." *Acoustica*, **71**, 1990.

[5] MP Felix, AT Ellis. "Laser-induced liquid breakdown: a step by step account." *Appl. Phys. Lett*. **19**, 1971.

[6] W Lautterborn, J Bolle. "Experimental investigations of cavitation-bubble collapse in the neighborhood of a solid boundary." *Fluid Mech*. **723**, (91) 1975.

[7] Royal Society of London, ed. "Joint European torus (JET)." *Philosophical Transactions of the Royal Society of London Series A*, **322**, (1563), 1986.

[8] NM Lawandy. "Interaction of charged particles on surfaces." *Appl. Phy. Lett*. **95** (234101-1-3), 2009.